

Hyperspherical calculations of ultralow-energy collisions in Coulomb three-body systems

Yueming Zhou,¹ Shinichi Watanabe,¹ Oleg I. Tolstikhin,² and Toru Morishita^{1,3}

¹*Department of Engineering Science, The University of Electro-Communications, 1-5-1 Chofu-ga-oka, Chofu-shi, Tokyo 182-8585, Japan*

²*Moscow Institute of Physics and Technology, Dolgoprudny 141700, Russia*

³*Institute for Advanced Science, The University of Electro-Communications, 1-5-1 Chofu-ga-oka, Chofu-shi, Tokyo 182-8585, Japan*

(Received 28 July 2015; published 28 September 2015)

Quantum mechanical calculations of ultralow-energy collision of Coulomb three-body systems in the hyperspherical elliptic coordinates are presented. The nonadiabatic coupling between the hyperradius and hyperangular variables is treated with the slow-variable discretization method in combination with the R -matrix propagation technique. For scattering state calculations, the two-dimensional matching procedure using Gailitis's method [M. Gailitis, *J. Phys. B* **9**, 843 (1976); C. Noble and R. Nesbet, *Comput. Phys. Commun.* **33**, 399 (1984)] is implemented to determine the boundary conditions between the internal and the asymptotic wave functions. This method is proved to be very efficient and gives very accurate results. Taking advantage of this method, we accurately calculate the scattering phase shifts and the scattering lengths of Coulomb three-body systems with mass ratio varying over several orders of magnitudes. We observed jumps of the scattering length from $-\infty$ to ∞ at certain mass ratios and monotonic decreases between two jumps. These are closely related to the binding energy of the highest bound state through Levinson's theorem [N. Levinson, *K. Dan. Vidensk. Selsk. Mat. Fys. Medd.* **25**, 9 (1949)]. Our calculations provide a comprehensive perspective to the scattering length from the variation of mass ratio of Coulomb three-body systems.

DOI: [10.1103/PhysRevA.92.032713](https://doi.org/10.1103/PhysRevA.92.032713)

PACS number(s): 34.10.+x, 36.10.-k, 34.50.-s

I. INTRODUCTION

The Coulomb three-body problem is fundamental to atomic and molecular physics as a basic component for understanding more complex many-body problems. This problem is not analytically solvable, but is still simple enough to be studied with accurate numerical results by advanced computational techniques. A number of theoretical studies have been devoted to accurate scattering calculations with different computational methods for various systems including prototypical systems of H^- [1], He [2–4], HD^+ [5], and H_2^+ [6] as well as exotic atoms such as Ps^- [7–10], $dt\mu$ [11,12], and $\bar{p}H$ [13]. In addition to those studies for each particular system, systematic investigations are very important for a deeper understanding of the underlying physics. A three-body system interacting via the Coulomb force is parametrized by the combinations of charges and masses of constituting particles. Physical quantities can be analyzed by continuously changing these parameters. For instance, the parameter region for the existence of stable bound states in Coulomb three-body systems has been explored [14,15]. It is known that only certain combinations of the masses of constituting particles with unit charge can have stable bound states. The boundary of the stability domain in the mass ratio space is examined using accurate variational calculations [15]. For resonance states, evolution of the wave function as a function of the mass ratio was analyzed from the hyperspherical point of view [16]. It is also shown that the resonance width oscillates over a wide range with the mass ratio due to the interference between two decaying paths [17]. Adiabatic quasiseparability of Coulomb three-body systems in the hyperspherical elliptic (HSE) coordinates [18] was analyzed in Ref. [19]. It has been demonstrated that the bound and resonance states for arbitrary charges and masses can be characterized by a set of approximate quantum numbers [19]. Such analyses indeed provide rich information on the stability of quantum many-body systems.

In this paper we report a systematic study of ultralow-energy collisions in Coulomb three-body systems. Recent progress in experimental techniques opened a new research field of cold collisions [20–22]. Knowledge of the cold collisions is essential for various physics communities, such as laser cooling and trapping [23], chemical reactions at ultralow energies [24], formation of Rydberg atoms and exotic atoms [25], and intense laser-atom interactions [26,27]. Indeed, several accurate calculations [28–31] in the ultralow-energy collision regime have been presented for several Coulomb three-body systems, but no systematic investigations so far.

We restrict ourselves to the analysis of symmetric Coulomb three-body systems consisting of singly charged particles, where two of the three are identical and the third particle has the opposite charge. The properties of these systems are uniquely characterized by the mass ratio \mathcal{M} of the constituting particles. The limit $\mathcal{M} \rightarrow 0$ of these systems is the atomic system H^- and the limit $\mathcal{M} \rightarrow \infty$ is the molecular system H_2^+ . Some other systems such as Ps^- correspond to a finite value of \mathcal{M} . We focus on the low-energy collisions between one of the two identical particles with the other pair in the ground state. We employ the HSE coordinate method [18,19] to obtain accurate phase shifts for a number of different \mathcal{M} values in the ultralow-energy regime. With the quasiseparability of Coulomb three-body systems in the HSE coordinates, observables are calculated very efficiently for arbitrary Coulomb three-body systems just by treating the charges and masses as input parameters.

The scattering length is a fundamental concept in ultracold collisions. It played an essential role in the blueshift and redshift of high Rydberg states of atoms in low-pressure gases [32]. Knowledge of it was also essential in the first creation of atomic Bose-Einstein condensate [33,34]. The Efimov states exist [35,36] in an anomalous situation when the two-body scattering length goes to infinity. As we will see

later, the scattering length jumps from $-\infty$ to ∞ many times while \mathcal{M} is increased continuously. We analyze those jumps by relating them to the binding energy of the highest bound state of the system. Our results give a comprehensive perspective to the ultralow-energy collisions from the variation of the mass ratio of Coulomb three-body systems.

This paper is organized as follows. The HSE coordinate method is recapitulated in Sec. II. Essential steps of the calculations are outlined. In Sec. III the results of the phase shifts for real physical systems, such as H^- , Ps^- , and H_2^+ , are compared with previous data obtained by other methods, confirming the accuracy of our method. Then the mass ratio dependence of the extracted scattering lengths is presented and discussed. Section IV summarizes the paper.

II. METHOD

We provide essential steps of the HSE coordinate method for bound- and continuum-state calculations. Detailed descriptions of the method can be found in previous papers [19,37]. In this section we consider a general three-body system with masses m_i and charges e_i ($i = 1, 2, 3$) interacting with each other by the Coulomb forces, although we will analyze only symmetric systems with $e_1 = e_2$ and $m_1 = m_2$. In this paper we use modified atomic units (m.a.u.), defined by $e_3 = m_3 = \hbar = 1$, which are suitable for considering a wide range of masses and charges at the same time. We also use the standard atomic units (a.u.) when a particular system is considered.

Let \mathbf{r}_i ($i = 1, 2, 3$) be the position of the i th particle in the center-of-mass frame. The mass scaled Jacobi coordinates are defined by

$$\mathbf{x}_i = \sqrt{M_i} \mathbf{r}_i, \quad (1)$$

$$\mathbf{y}_i = \sqrt{\mu_i} (\mathbf{r}_{i+2} - \mathbf{r}_{i+1}), \quad (2)$$

where

$$M_i = \frac{m_i(m_{i+1} + m_{i+2})}{m_i + m_{i+1} + m_{i+2}}, \quad \mu_i = \frac{m_{i+1}m_{i+2}}{m_{i+1} + m_{i+2}} \quad (3)$$

are the reduced masses and $\{i, i+1, i+2\}$ denote a cyclic permutation of $\{1, 2, 3\}$. The three sets of Jacobi coordinates are related by the kinematic rotation

$$\begin{bmatrix} \mathbf{x}_{i+2} \\ \mathbf{y}_{i+2} \end{bmatrix} = \begin{bmatrix} -\cos \gamma_i & -\sin \gamma_i \\ \sin \gamma_i & -\cos \gamma_i \end{bmatrix} \begin{bmatrix} \mathbf{x}_{i+1} \\ \mathbf{y}_{i+1} \end{bmatrix}, \quad (4)$$

with the kinematic rotation angles given by

$$\tan \gamma_i = \sqrt{\frac{m_i(m_1 + m_2 + m_3)}{m_{i+1}m_{i+2}}}, \quad 0 \leq \gamma_i \leq \pi/2. \quad (5)$$

In the HSE coordinates, the six degrees of freedom of the three-body system are described by the hyperradius

$$R = \sqrt{x_i^2 + y_i^2} = \left(\sum_{i=1}^3 m_i r_i^2 \right)^{1/2}, \quad (6)$$

which measures the size of the system, and five hyperangles symbolically represented by Ω , which define the relative positions of the three particles. The hyperangles Ω can be split into two parts Ω_E and Ω_S . The former Ω_E represents the

three Euler angles defining the orientation of the three-body system with respect to the laboratory fixed frame and Ω_S represents two variables parametrizing the shape of the three-body triangle. Since we focus on the ultralow-energy collision, we only consider the system with zero total angular momentum $J = 0$. In this case, the Euler angles can be eliminated and thus the six-dimensional problem is reduced to a three-dimensional one with variables R and Ω_S . In the HSE coordinates, the two shape angles Ω_S are defined by [18]

$$\eta_i = \chi_{i+1} - \chi_{i+2}, \quad -2\gamma_i \leq \eta_i \leq 2\gamma_i, \quad (7)$$

$$\xi_i = \chi_{i+1} + \chi_{i+2}, \quad 2\gamma_i \leq \xi_i \leq 2\pi - 2\gamma_i, \quad (8)$$

where $\{\chi_i\}$ are the so-called Delves hyperangles

$$\tan \frac{\chi_i}{2} = \frac{y_i}{x_i}, \quad 0 \leq \chi_i \leq \pi. \quad (9)$$

In what follows we use $\Omega_S = (\eta_3, \xi_3)$ for shape angles and for simplicity omit the subscript. The Schrödinger equation for $J = 0$ in the HSE coordinates is then written as

$$\left(-\frac{1}{2} \frac{1}{R^5} \frac{\partial}{\partial R} R^5 \frac{\partial}{\partial R} + \frac{\Lambda^2(\Omega_S)}{2R^2} + \frac{C(\Omega_S)}{R} - E \right) \times \Psi(R, \Omega_S) = 0, \quad (10)$$

where $C(\Omega_S)$ is the effective charge and $\Lambda^2(\Omega_S)$ is the square of the grand angular momentum operator. The explicit forms of $C(\Omega_S)$ and $\Lambda^2(\Omega_S)$ in the HSE coordinates are

$$\Lambda^2(\eta, \xi) = -\frac{16}{\cos \eta - \cos \xi} \left[\frac{\partial}{\partial \eta} (\cos \eta - \cos 2\gamma) \frac{\partial}{\partial \eta} + \frac{\partial}{\partial \xi} (\cos 2\gamma - \cos \xi) \frac{\partial}{\partial \xi} \right], \quad (11)$$

$$C(\eta, \xi) = 4 \frac{\cos(\eta/2) + \cos(\xi/2)}{\cos \eta - \cos \xi} \times \left[z^+ \cos \frac{\eta}{4} \sin \frac{\xi}{4} + z^- \sin \frac{\eta}{4} \cos \frac{\xi}{4} \right] + \frac{\sqrt{2}z_3}{\sqrt{1+p^+ \cos(\eta/2) \cos(\xi/2) - p^- \sin(\eta/2) \sin(\xi/2)}}, \quad (12)$$

where

$$z_i = e_{i+1}e_{i+2}\sqrt{\mu_i}, \quad z^\pm = z_2 \pm z_1 \quad (13)$$

and

$$p^+ = 1 + \frac{2m_3}{m_1 + m_2}, \quad p^- = \frac{m_2 - m_1}{m_1 + m_2}. \quad (14)$$

One of the basic ideas of the hyperspherical method is the adiabatic separation between R and Ω_S [38,39]. The crucial step is to solve the two-dimensional (2D) adiabatic eigenvalue problem (EVP)

$$[H_{\text{ad}}(R) - U_\nu(R)]\Phi_\nu(\Omega_S; R) = 0, \quad (15)$$

where

$$H_{\text{ad}}(R) = \frac{1}{2} \Lambda^2(\Omega_S) + RC(\Omega_S) \quad (16)$$

is the adiabatic Hamiltonian, which is an operator in Ω_S and depends parametrically on R . The eigenvalues $U_\nu(R)$

and the associated eigenfunctions $\Phi_v(\Omega_S; R)$ are called the hyperspherical potentials and the adiabatic channel functions, respectively. Following Refs. [18,19], we adopt a two-step procedure based on the splitting of the effective charge into two parts

$$C(\eta, \xi) = C_s(\eta, \xi) + C_r(\eta, \xi), \quad (17)$$

where $C_s(\eta, \xi)$ and $C_r(\eta, \xi)$ are the separable and the residual parts, respectively, and their explicit forms are given in Ref. [19]. First, we solve the separable EVP in Eq. (15), where $C(\eta, \xi)$ is replaced by $C_s(\eta, \xi)$. The 2D EVP then consists of a pair of two 1D EVPs, which can be solved much more easily with the discrete-variable representation (DVR) method. In the second step, we use the direct products of the separable basis sets generated in the previous step for solving the 2D adiabatic EVP in Eq. (15). It has been shown that for Coulomb three-body systems, the contributions of C_r can be minimized systematically and the number of basis functions in the second step of diagonalization can be significantly reduced. This quasiseparability using η and ξ is of great advantage to numerical calculations with the HSE coordinates. A complete analysis of the quasiseparability for Coulomb three-body systems is given in Ref. [18].

For the symmetric systems, the solutions of Eq. (10) can be separated into either even or odd states under the permutation of the two identical particles 1 and 2. In the HSE coordinates, the permutation is represented by the exchange of η and $-\eta$. We separately calculate the even and odd states in Eq. (15) by choosing symmetric and antisymmetric basis sets with respect to $\eta = 0$. As examples, the lowest 100 hyperspherical adiabatic potentials of Ps^- with even and odd symmetries are shown in Figs. 1(a) and 1(b), respectively.

Having $U_v(R)$ and $\Phi_\mu(\Omega_S; R)$, we next solve the coupled equations in R . Substituting a different function defined by

$$\psi(R, \Omega_S) = R^{3/2} \Psi(R, \Omega_S) \quad (18)$$

into Eq. (10), we obtain

$$[K(R) + H_{\text{ad}}(\Omega_S; R) - R^2 E] \psi(R, \Omega_S) = 0, \quad (19)$$

where

$$K(R) = -\frac{1}{2} \frac{\partial}{\partial R} R^2 \frac{\partial}{\partial R} + \frac{15}{8} \quad (20)$$

corresponds to the kinetic energy operator for the motion in R . We use slightly different procedures for bound and continuum states.

For bound-state calculations we solve Eq. (19) with the slow-variable discretization (SVD) method [40]. In this method the wave function is expanded as

$$\psi_n(R, \Omega_S) = \sum_{i=1}^{N_{\text{DVR}}} \sum_{v=1}^{N_{\text{ch}}} C_{iv}^n \pi_i(R) \Phi_v(\Omega_S; R_i), \quad (21)$$

where $\pi_i(R)$ ($R \in [0, \infty]$) are the DVR basis functions constructed from the associated Laguerre polynomials and indexed by the DVR quadrature points R_i . Substituting Eq. (21) into Eq. (19), we arrive at the SVD algebraic EVP

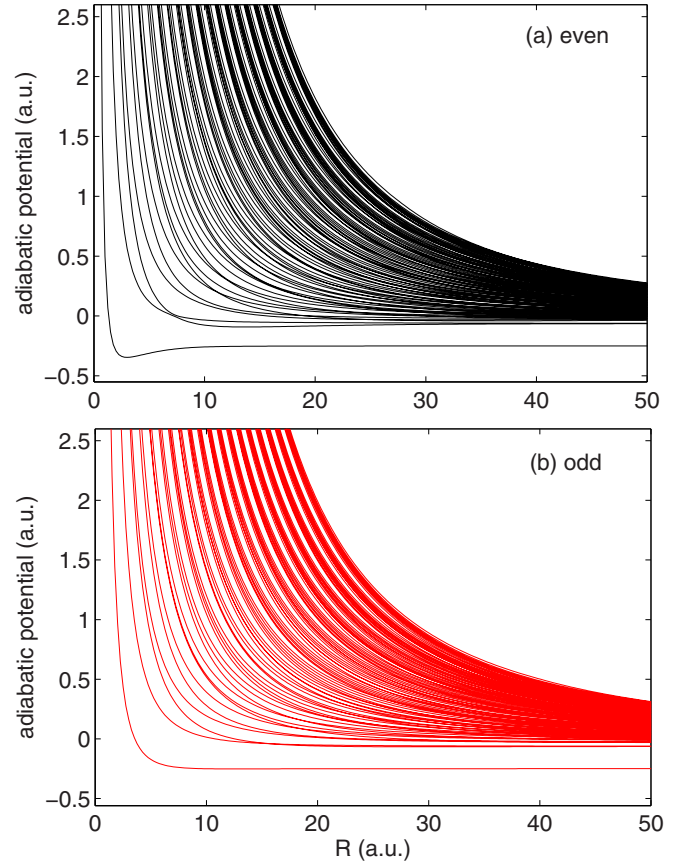


FIG. 1. (Color online) Hyperspherical adiabatic potentials $[U_v(R) + 15/8]/R^2$ for Ps^- with (a) even and (b) odd permutation symmetries.

defining the coefficients C_{iv}^n and eigenvalues E_n ,

$$\sum_{j=1}^{N_{\text{DVR}}} \sum_{\mu=1}^{N_{\text{ch}}} \{K_{ij} O_{iv, j\mu} + R_i^2 [U_v(R_i) - E_n] \delta_{ij} \delta_{v\mu}\} C_{j\mu}^n = 0, \quad (22)$$

where N_{DVR} and N_{ch} are the numbers of the hyperradial DVR basis set and of the adiabatic channels included in the calculations, respectively. The total dimension of the basis set for the SVD EVP is $N_{\text{SVD}} = N_{\text{DVR}} \times N_{\text{ch}}$. In Eq. (22)

$$K_{ij} = \frac{1}{2} \int_0^\infty \frac{d\pi_i(R)}{dR} R^2 \frac{d\pi_j(R)}{dR} dR + \frac{15}{8} \delta_{ij} \quad (23)$$

is the DVR matrix for the operator $K(R)$ and

$$O_{iv, j\mu} = \langle \Phi_v(\Omega_S; R_i) | \Phi_\mu(\Omega_S; R_j) \rangle \quad (24)$$

is the overlap matrix. Here $\langle \dots | \dots \rangle$ denotes the integration over η and ξ .

In order to obtain very accurate results, we should include a large number of adiabatic channels that may have strong nonadiabatic couplings near the sharp avoided crossings as shown in Fig. 1. The SVD method implicitly incorporates the nonadiabatic couplings among the adiabatic channels in an algebraic form using the overlap matrix elements at the DVR quadrature points.

For scattering state calculations, Eq. (19) should be solved from $R = 0$ to the matching hyperradius $R = R_m$ and matched to the asymptotic solutions to extract scattering information. The interval $[0, R_m]$ is divided into a number of sectors and within each sector the equations are solved using the SVD method. We then employ the R -matrix propagation [41] from sector to sector. This combined method of SVD and R -matrix propagation was first introduced in treating electron impact ionization of hydrogen [4] and atom transfer reactions in atom-diatom collisions [37] where its accuracy and efficiency were confirmed. Then it was used in other Coulomb three-body systems, such as $dt\mu$ [11]. Very recently, this method was also employed in the recombination processes of three identical bosons [42] and the elastic and reactive atom-molecule collisions [43]. In this R -matrix propagation procedure, we consider the kinetic energy operator in the k th sector between R_{k-1} and R_k , amended by the Bloch operator $L(R)$, namely,

$$\tilde{K}(R) = K(R) + L(R), \quad (25)$$

where

$$L(R) = \frac{1}{2}R^2[\delta(R - R_k) - \delta(R - R_{k-1})]\frac{\partial}{\partial R}. \quad (26)$$

The Bloch operator is introduced here to make the operator $\tilde{K}(R)$ Hermitian. Within each sector, we solve Eq. (19) with $K(R)$ replaced by $\tilde{K}(R)$,

$$[\tilde{K}(R) + H_{\text{ad}}(\Omega_S; R) - R^2\tilde{E}]\tilde{\psi}(R, \Omega_S) = 0 \quad (27)$$

with the SVD expansion as in Eq. (21),

$$\tilde{\psi}_n(R, \Omega_S) = \sum_{i=1}^{N_{\text{DVR}}} \sum_{v=1}^{N_{\text{ch}}} \tilde{C}_{iv}^n \pi_i(R) \Phi_v(\Omega_S; R_i), \quad (28)$$

$$V = \frac{\sqrt{\mu_i} e_{i+1} e_{i+2}}{y_i} + \frac{\sqrt{M_i} e_i}{x_i} \sum_{l=0}^{\infty} \left[e_{i+2} \left(\frac{y_i}{x_i \tan \gamma_{i+2}} \right)^l + e_{i+1} \left(\frac{-y_i}{x_i \tan \gamma_{i+1}} \right)^l \right] P_l(\cos \theta_i), \quad (33)$$

where $P_l(\cos \theta_i)$ are the Legendre polynomials, θ_i is the angle between \mathbf{x}_i and \mathbf{y}_i . The first term of Eq. (33) is the Coulomb interaction of the bound pair and the second part of the sum over $l = 0, 1, \dots$ corresponds to the multipole expansion of the potential between the i th particle and the bound pair. Retaining only $0 \leq l \leq l_{\text{max}}$ terms in the expansion in Eq. (33), we get

$$\left[-\frac{\Delta y_i}{2} - \frac{\Delta x_i}{2} + \frac{\sqrt{\mu_i} e_{i+1} e_{i+2}}{y_i} + \frac{\sqrt{M_i} e_i (e_{i+1} + e_{i+2})}{x_i} + \sum_{l=1}^{l_{\text{max}}} A_l - E \right] \Psi_{\text{as}}(\mathbf{x}_i, \mathbf{y}_i) = 0, \quad (34)$$

where

$$A_l = \sqrt{M_i} e_i \left[e_{i+2} \left(\frac{1}{\tan \gamma_{i+2}} \right)^l + e_{i+1} \left(\frac{-1}{\tan \gamma_{i+1}} \right)^l \right] \frac{y_i^l}{x_i^{l+1}} P_l(\cos \theta_i). \quad (35)$$

The solutions to Eq. (34) can be written as

$$\Psi_{\mu_{\text{as}}}^{(S,C)}(\mathbf{x}_i, \mathbf{y}_i) = R^{3/2} \sum_{\nu_{\text{as}}} \frac{1}{x_i \sqrt{k_{\nu_{\text{as}}}}} F_{\nu_{\text{as}} \mu_{\text{as}}}^{(S,C)}(x_i, k_{\nu_{\text{as}}}) B_{\nu_{\text{as}}}(\mathbf{y}_i). \quad (36)$$

Here

$$B_{\nu_{\text{as}}}(\mathbf{y}_i) = \frac{1}{y_i} \varphi_{\nu_j}(y_i) P_j(\cos \theta_i) \quad (37)$$

is the asymptotic channel function, which describes the motion of the i th bound pair with a collective index $\nu_{\text{as}} = \{\nu, j\}$,

where $\pi_i(R)$ is the DVR basis set associated with the Legendre polynomials. Then the R matrix \mathcal{R} defined by

$$\begin{aligned} & \langle \Phi_\nu(\Omega_S; R) | \psi(R; \Omega_S) \rangle \\ &= \sum_{\mu} \mathcal{R}_{\nu\mu}(R) \left\langle \Phi_\nu(\Omega_S; R) \left| \frac{\partial \psi(R; \Omega_S)}{\partial R} \right. \right\rangle \end{aligned} \quad (29)$$

is propagated from R_{k-1} to R_k across the boundary using

$$\mathcal{R}(R_k) = \mathcal{R}^{kk} - \mathcal{R}^{kk-1} [\mathcal{R}^{k-1k-1} + \mathcal{R}(R_{k-1})]^{-1} \mathcal{R}^{k-1k}, \quad (30)$$

where

$$\mathcal{R}_{\nu\mu}^{kl} = \frac{1}{2} \sum_{n=1}^{N_{\text{SVD}}} \frac{\tilde{F}_{\nu n}(R_k) \tilde{F}_{\mu n}(R_l)}{\tilde{E}_n - E} \quad (31)$$

and

$$\tilde{F}_{\nu n}(R_a) = R_a \langle \Phi_\nu(\Omega_S; R_a) | \tilde{\psi}_n(R_a, \Omega_S) \rangle. \quad (32)$$

In Eq. (31) \tilde{E}_n are the eigenvalues of Eq. (27) and in Eq. (32) R_a stands for either R_{k-1} or R_k . We repeat this procedure from the first sector with $\mathcal{R}(R = 0) = 0$ to the last sector to obtain the R matrix at the matching radius $\mathcal{R}(R = R_m)$. This step constructs the solutions in the interior region.

In our scattering calculations, the asymptotic wave functions are expressed in the mass-scaled Jacobi coordinates [37]. In the limit of $x_i \gg y_i$ the potential energy of the three-body system is expanded in (x_i, y_i) coordinates as

describing ν and j as the principle and angular quantum numbers of the bound pair, respectively, and $\varphi_{\nu_j}(y_i)$ is the solution to the radial equation

$$\left[\frac{d^2}{dy_i^2} + 2\mu_i \left(\varepsilon_{\nu_j} - \frac{\sqrt{\mu_i} e_{i+1} e_{i+2}}{y_i} \right) - \frac{j(j+1)}{y_i^2} \right] \varphi_{\nu_j}(y_i) = 0, \quad (38)$$

with the boundary conditions

$$\varphi_{\nu_j}(0) = \varphi_{\nu_j}(\infty) = 0. \quad (39)$$

In Eq. (37) $\varepsilon_{vj} < 0$ is the bound-state energy of the bound pair in the $v_{\text{as}} = \{v, j\}$ channel. The relative motion of the i th particle and the i th bound pair is described by $\frac{1}{x_i \sqrt{k_{v_{\text{as}}}}} F_{v_{\text{as}} \mu_{\text{as}}}^{(S,C)}(x_i, k_{v_{\text{as}}})$

in Eq. (36) with $F_{v_{\text{as}} \mu_{\text{as}}}^{(S,C)}(x_i, k_{v_{\text{as}}})$ being the regular S and irregular C solutions of the equation

$$\left[\frac{d^2}{dx_i^2} - \frac{j(j+1)}{x_i^2} - \frac{2\sqrt{M_i} e_i (e_{i+1} + e_{i+2})}{x_i} + k_{\mu_{\text{as}}}^2 \right] F_{\mu_{\text{as}}}(x_i) = \sum_{v_{\text{as}}} \sum_{l=1}^{l_{\text{max}}} \frac{A_{v_{\text{as}} \mu_{\text{as}}}^l}{x_i^{l+1}} F_{v_{\text{as}}}(x_i), \quad (40)$$

where

$$k_{\mu_{\text{as}}} = \sqrt{2M_i(E - \varepsilon_{\mu_{\text{as}}})} \quad (41)$$

are the asymptotic momenta, describing the relative momenta between the incident particle and the target system, and

$$A_{\mu_{\text{as}} v_{\text{as}}}^l = \int B_{\mu_{\text{as}}}(\mathbf{y}_i) A_l B_{v_{\text{as}}}(\mathbf{y}_i) d\mathbf{y}_i \quad (42)$$

is the matrix of the multipole couplings. Equation (40) is solved using Gailitis's method [44,45] with proper boundary conditions at $x_i \rightarrow \infty$ for open and closed channels and we found that it is sufficient to set $l_{\text{max}} = 1$ for the systems considered here.

We now implement the 2D matching to extract scattering information [37]. Matching requires that the function and its derivative solved with the SVD and R -matrix propagation methods for $R \leq R_m$ and those obtained with Gailitis's method for $R \geq R_m$ coincide at the hyperspherical surface $R = R_m$. Projecting these conditions on the hyperspherical channel functions by performing the integral over the hyperangles η and ξ , the \mathbf{K} matrix is given by

$$\mathbf{K} = -(\mathbf{F}^{(C)} - \mathcal{R}\mathbf{D}^{(C)})^{-1}(\mathbf{F}^{(S)} - \mathcal{R}\mathbf{D}^{(S)}), \quad (43)$$

where

$$\mathbf{F}_{v_{\text{as}}}^{(S,C)} = \langle \Phi_v(\Omega_S; R) | \Psi^{(S,C)} \rangle_{R=R_m}, \quad (44)$$

$$\mathbf{D}_{v_{\text{as}}}^{(S,C)} = \left\langle \Phi_v(\Omega_S; R) \left| \frac{\partial \Psi^{(S,C)}}{\partial R} \right. \right\rangle_{R=R_m}. \quad (45)$$

The advantage of the 2D matching is that the scattering information can be extracted with a smaller matching radius and thus the computational demand in the calculations for the interior region can be significantly reduced. It has been widely used in the hyperspherical approach and its accuracy has been confirmed in [2,4,11,37,46].

For the ultralow-energy regime, there is only one open channel. In this situation the matrix (43) is a number $\mathbf{K} = K$ and the phase shift

$$\delta = \arctan K. \quad (46)$$

Convergence of the calculations strongly depends on the system. In the bound-state calculations, we introduce a scaling parameter in the hyperradial grid in such a way that the largest DVR quadrature point $R_{i=N_{\text{DVR}}} = R_{\text{max}}$. Then we check the convergence of the bound-state energies by increasing N_{DVR} . For H^- as a typical system of $\mathcal{M} \sim 0$, $R_{\text{max}} = 50$ a.u. and $N_{\text{DVR}} = 30$ together with $N_{\text{ch}} = 30$ in the SVD expansion

[see Eq. (22)] are large enough to obtain the accuracy of eight significant digits in the bound-state energies. For Ps^- with $\mathcal{M} = 1$, $R_{\text{max}} = 100$ a.u., $N_{\text{DVR}} = 30$, and $N_{\text{ch}} = 30$ are used. For systems with large \mathcal{M} , especially for those with a very weakly bound state, larger R_{max} and N_{DVR} are needed, while N_{ch} can be reduced. For example, for H_2^+ , $R_{\text{max}} = 3500$ a.u. and $N_{\text{ch}} = 10$ are enough to obtain converged bound-state energies. For the scattering calculations, the main factor influencing convergence is the matching radius R_m . For H^- , $R_m = 100$ a.u. is large enough to reach accurate results. For H_2^+ , R_m should be larger than 10^4 a.u., if we aim to extract the scattering length at ultralow collision energies. We also carefully check the accuracy of the adiabatic channel function by increasing the number of DVR quadrature points in η and ξ particularly at large R . For H^- , with $R = 100$ a.u., we used 200 quadrature points in each of η and ξ . We have checked that this number ensures the accuracy of nine digits in the adiabatic potentials. For H_2^+ with $R = 10^4$ a.u., the quadrature points in η and ξ required are 800 to reach this accuracy. In the SVD procedure for the scattering calculations, larger N_{ch} are needed compared to the bound-state calculations. Thus $N_{\text{ch}} = 135$ for H^- and 100 for H_2^+ are included. The convergence has been checked by enlarging these parameters for all the systems considered in this work.

III. RESULTS AND DISCUSSION

We consider symmetric Coulomb three-body systems with positive and negative unit charges, i.e., $\pm e_1 = \pm e_2 = \mp e_3 = 1$ and $m_1 = m_2$. These systems can be characterized by the mass ratio $\mathcal{M} = m_1/m_3 = m_2/m_3$. First we will present the numerical results of the phase shifts δ at several collision energies and the scattering length a for some realistic systems and compare them with previous data calculated with other methods. Then we will analyze the scattering length $a(\mathcal{M})$ by changing \mathcal{M} continuously in a wide range to study ultralow-energy collisions.

A. Comparison with preceding results

For the low-energy collisions here, there is only one open channel for both even and odd symmetries, corresponding to the collisions of a particle with the others in their ground state. In Table I we compare our results of the phase shifts in both symmetries with other available data for the $e\text{-H}$ (H^-), $e\text{-Ps}$ (Ps^-), and $p\text{-H}$ (H_2^+) collisions, which are prototypes of $\mathcal{M} \rightarrow 0$, $\mathcal{M} \sim 1$, and $\mathcal{M} \rightarrow \infty$, respectively. The relative momenta between the incident particle and the target system in Eq. (41) in a.u. are indicated as

$$k = \sqrt{2M_1(E + \mu_1/2)}, \quad (47)$$

where E is the total energy measured from the breakup threshold, defined in Eq. (10), and $-\mu_1/2$ represents the ground-state energy of the target. The H^- system has been widely studied with various methods. In this table we compare our results with the results from the variational methods [1,47], the complex-correlation Kohn T -matrix method [48], and the Siegert pseudostate method [49]. It is shown that our results agree well with those for both even and odd permutation symmetries. Note that in our calculations and in Ref. [49]

TABLE I. Comparison of phase shifts (in radians) of H^- , Ps^- , and H_2^+ . For H^- , the mass of the proton in our calculation and Ref. [49] is set to be 1836.1527 a.u., while in Refs. [1,47,48] it is infinite. The numbers in the parentheses give the uncertainty in the last digit.

H^-					
k (a.u.)	Present work	Ref. [49]	Ref. [1]	Ref. [47]	Ref. [48]
Even					
0.1	2.5531	2.5532	2.553(1)	2.5561	2.5536
0.2	2.0661	2.0663	2.0673(9)	2.0666	2.0668
0.3	1.6957	1.6961	1.6964(5)	1.6963	1.6982
0.4	1.4143	1.4149	1.4146(4)	1.4152	1.4154
0.5	1.1998	1.2004	1.202(1)	1.2010	1.2009
0.6	1.0398	1.0404	1.041(1)	1.0408	1.0408
0.7	0.9296	0.9303	0.930(1)	0.9303	0.9311
0.8	0.8867	0.8873	0.886(1)	0.8870	0.8872
Odd					
0.1	2.9383		2.9388(4)	2.9385	2.9385
0.2	2.7170		2.7171(5)	2.7174	2.7174
0.3	2.4991		2.4996(8)	2.4997	2.4998
0.4	2.2933		2.2938(4)	2.2941	2.2941
0.5	2.1037		2.1046(4)	2.1046	2.1045
0.6	1.9320		1.9329(8)	1.9328	1.9327
0.7	1.7785		1.7797(6)	1.7794	1.7795
0.8	1.6429		1.643(3)	1.6438	1.6438
Ps^-					
k (a.u.)	Present work	Ref. [7]	Ref. [8]	Ref. [9]	Ref. [10]
Even					
0.1	2.0557	2.049	2.062	2.056	1.894
0.2	1.3782	1.378	1.386	1.378	1.226
0.3	0.9828	0.984	0.989	0.983	0.876
0.4	0.7455	0.748	0.751	0.746	0.643
Odd					
0.1	2.6052	2.605	2.608	2.6056	2.596
0.2	2.1074	2.106	2.111	2.1086	2.105
0.3	1.7105	1.709	1.714	1.7116	1.720
0.4	1.4040	1.402	1.412	1.4056	1.409
H_2^+					
Energy (eV)	Even		Odd		
	Present work	Ref. [52]	Present work	Ref. [52]	
0.0001	1.1011	1.1058	2.2759	2.2758	
0.0002	0.3610	0.3643	1.5758	1.5757	
0.0003	3.0019	3.0036	1.0922	1.0921	
0.0005	2.2878	2.2874	0.3960	0.3957	
0.0007	1.7586	1.7567	3.0210	3.0204	
0.0010	1.1382	1.1345	2.4176	2.4163	
0.0015	0.3475	0.3420	1.6537	1.6516	
0.0020	2.8655	2.8590	1.0549	1.0530	

the proton mass is set to 1836.1527 a.u., while it is infinite in the other calculations. We also implemented the calculations with a very large proton mass of 10^6 a.u. and found that the results indeed get closer to those of Refs. [47,48], but there still exist small discrepancies in the fourth decimal places.

For the e - Ps collision the results from the variational method [7], close-coupling method [9,10], and by directly solving the modified Faddeev equations [8] are shown for comparison. A good agreement is achieved with these accurate calculations.

TABLE II. Phase shifts (in radians) of H_2^+ .

k (a.u.)	Even	Odd
0.1	0.6985	1.8974
0.2	2.0269	0.1410
0.3	0.5872	1.8846
0.4	2.4701	0.6764
0.5	1.3260	2.7264
0.6	0.2643	1.7151
0.7	2.4076	0.7635
0.8	1.4603	3.0008

For the p - H case, only limited data are available at low collision energies. Moreover, the Born-Oppenheimer (BO) approximation is often used to study the ion-atom collisions. However, it has been shown that the BO approximation breaks down for ultralow-energy collisions [50,51]. Hunter and Kuriyan obtained the phase shifts for p - H collision at low energies within the BO approximation including nonadiabatic correction to the BO potentials [52]. These are the only data we know of for this system. The good agreement of these data with the present fully nonadiabatic results supports the high accuracy of the BO approximation. In Table II we include more data on the p - H collision for reference in future studies.

We now focus our attention on the scattering length a , which is a property of each collision system in the low-energy limit. We extract the values of a from the calculated phase shifts δ by fitting to the effective range expansion [53]

$$k \cot \delta = -\frac{1}{a} + bk + ck^2 \ln k, \quad (48)$$

where coefficients b and c are also determined by the fitting. Table III lists the extracted a of various systems for even and odd symmetries from our calculations. Benchmark results from the variational methods [1,7] for H^- and Ps^- are also shown. Our results of H^- agree with the variational calculations within a few percent, but are slightly larger for both even and odd symmetries. Note that the proton mass of 1836.1527 a.u. is used in our calculations, while it is infinite in Ref. [1]. By increasing the mass of proton and extrapolation,

TABLE III. Scattering lengths in a.u. for realistic physical systems. The masses of the muon, proton, deuteron, and tritium are 206.768 26, 1836.1527, 3670.4830, and 5496.9216 a.u., respectively.

	Even		Odd	
	Present work	Other works	Present work	Other works
H^-	6.02	5.965 ± 0.003^a	1.82	1.7686 ± 0.0002^a
Ps^-	11.88	12.0 ± 0.3^b	4.77	4.6 ± 0.4^b
H_2^+	-31.0	-28.8^c -29.3^d	715.0	725.2^c 750^d
$pp\mu$	-1.455×10^{-1}		1.736×10^{-2}	
$dd\mu$	2.467×10^{-2}		1.519×10^{-2}	
$tt\mu$	-4.169×10^{-2}		1.228×10^{-2}	

^aReference [1].

^bReference [7].

^cReference [54].

^dReference [55].

we obtain $a = 6.01$ a.u. for H^- with infinite proton mass. Thus the differences in a are not attributable to the different masses used in the two methods. For Ps^- , the results also agree well with the variational calculations in [7] within the reported uncertainties. For H_2^+ , no variational calculations are available. We show in Table III the results based on the modified BO approximation [54] and from the Faddeev equation [55] for comparison and found that the differences among the three calculations are several percent.

The results shown above establish the accuracy of our HSE coordinate method for the low-energy phase shifts as well as the scattering lengths in a wide range of mass ratio \mathcal{M} from $\sim 10^{-3}$ to $\sim 10^3$. We also present the calculated values of the scattering lengths for the other realistic systems of $pp\mu$, $dd\mu$, and $tt\mu$ in Table III for future reference.

B. Mass-ratio dependence of the scattering length

1. Even permutation systems

In order to get a deeper insight into the underlying physics of the mass ratio dependence of the scattering length, we calculate $a(\mathcal{M})$ for several systems by varying \mathcal{M} . In this section we use m.a.u. for the purpose of our systematic study. Note that the conversion of the scattering lengths from atomic units to the modified atomic units is given by a (m.a.u.) = $m_3 a$ (a.u.). The results for the even states are shown in Fig. 2(a) in the region of $\mathcal{M} = 0$ –2000 and they are distributed in a wide range of positive and negative values. According to Levinson's theorem [56] for potential scattering problems, the zero-energy phase shift can be expressed using the number of bound states

N_b , namely,

$$\delta(k=0) = N_b \pi \quad (49)$$

$$= (N_b + \frac{1}{2})\pi \quad (\text{if there is a half bound state of zero energy}). \quad (50)$$

Levinson's theorem implies that as the potential parameter changes continuously, the zero-energy phase shift increases by π when a new bound state appears. As a result, scattering length evolves from ∞ to $-\infty$ with the changing value of the potential parameter. This feature can be generalized to multichannel problems [57] such as the symmetric Coulomb three-body systems with \mathcal{M} as the parameter that changes continuously. In the following we examine the behavior of $a(\mathcal{M})$ based on the dependence of $N_b(\mathcal{M})$.

Figure 2(b) shows $N_b(\mathcal{M})$ for the even states; $N_b(\mathcal{M})$ increases monotonically from 1 to 21 when \mathcal{M} varies from 0 to 2000. We note $N_b = 1$ for H^- where $\mathcal{M} \sim 0$ and $N_b = 20$ for H_2^+ where $\mathcal{M} = 1836.1527$. We also plot the semiclassical estimate given by [58]

$$N_b = \left[\frac{S}{\pi} + \frac{1}{2} \right], \quad (51)$$

where $[x]$ denotes the integer part of x and S is the semiclassical action in m.a.u. estimated using the BO approximation

$$S = \int_{\rho_0}^{\infty} \sqrt{2\mathcal{M}[-\frac{1}{2} - U(\rho)]} d\rho = \alpha \sqrt{\mathcal{M}}. \quad (52)$$

Here $U(\rho)$ is the lowest BO potential for particle 3 in the two-center Coulomb potential with ρ being the distance between the two identical particles 1 and 2. The lower bound ρ_0 of the integral in Eq. (52) is the turning point where $U(\rho_0)$ coincides with the dissociation threshold of $-1/2$ m.a.u. in the BO approximation. Since $U(\rho)$ and ρ_0 are common for all the cases, the action S can be factorized into $\sqrt{\mathcal{M}}$ and a constant α that is determined by the potential. We obtain $\alpha = 1.4729$ for the even states by the numerical integration of the BO potential. Figure 2(b) indicates that the semiclassical BO approximation from Eqs. (51) and (52) provides a good estimate of N_b in a wide range of \mathcal{M} except for $\mathcal{M} \lesssim 1$, where the BO picture breaks down [see the inset of Fig. 2(b)]. From the behavior of $N_b(\mathcal{M})$ in Fig. 2(b) we expect that $a(\mathcal{M})$ would jump from $-\infty$ to ∞ 20 times near the locations where N_b has 20 steps in the range of $0 \leq \mathcal{M} \leq 2000$.

Figure 3 displays an expanded view of Fig. 2(a) in the range of $0 < \mathcal{M} \leq 35$, where several realistic systems exist. In this region, as can be seen in Fig. 3(b), the second and third bound states appear at $\mathcal{M} \sim 10$ and $\mathcal{M} \sim 30$, which are close to the semiclassical BO predictions of $\mathcal{M} = 10.6$ and $\mathcal{M} = 29.3$ from Eqs. (51) and (52), respectively. The corresponding scattering lengths $a(\mathcal{M})$ of these systems are shown in Fig. 3(a). Indeed, $a(\mathcal{M})$ has jumps from $-\infty$ to ∞ at the same locations, where the new bound states appear, and it decreases monotonically from ∞ to $-\infty$ in the range between the two jumps. In order to see this behavior more quantitatively, we estimate $a(\mathcal{M})$ from the relation derived from the analytic

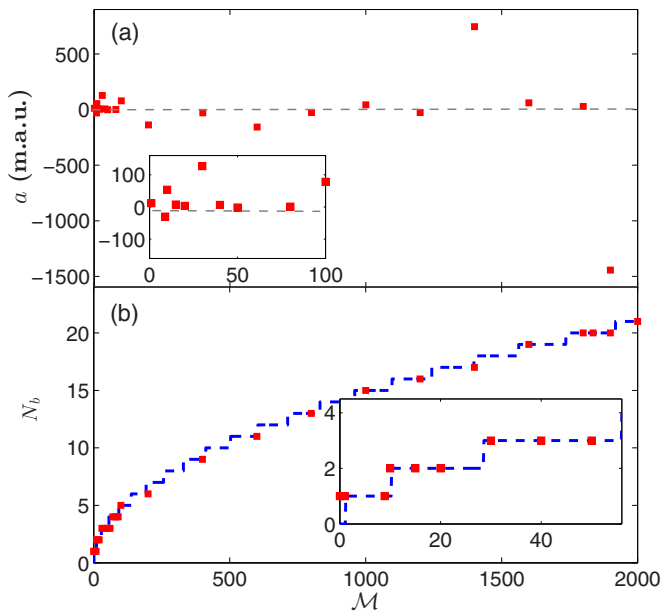


FIG. 2. (Color online) Mass ratio \mathcal{M} dependence of (a) scattering length a and (b) number of bound states N_b for even permutation states. The dashed line in (b) shows the results calculated from the semiclassical method in Eqs. (51) and (52). The insets show an expanded view of the small- \mathcal{M} region.

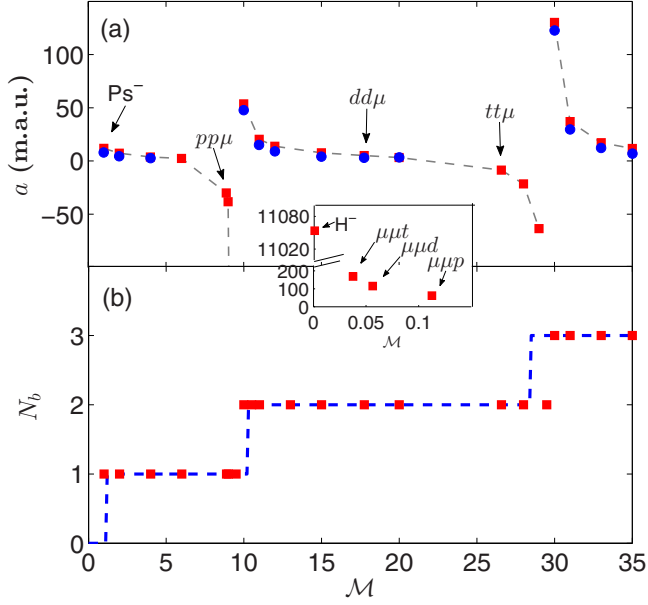


FIG. 3. (Color online) Mass-ratio \mathcal{M} dependence of (a) scattering length a and (b) number of bound states N_b for even permutation symmetry states in the range of $0 < \mathcal{M} \leq 35$. The blue dots in (a) are the results calculated with formula (53). The dashed line in (b) shows the results calculated from the semiclassical method using Eqs. (51) and (52). The inset shows the scattering lengths of some of the realistic systems with $\mathcal{M} \sim 0$.

continuation of the scattering amplitude [58],

$$a = \frac{1}{\sqrt{-2M_1 E_b}}, \quad (53)$$

where $M_1 = \mathcal{M}(\mathcal{M} + 1)/(2\mathcal{M} + 1)$ is the reduced mass defined in Eq. (3) in m.a.u. and $E_b < 0$ (m.a.u.) is the binding energy of the highest bound state measured from the lowest dissociation threshold of $-\mu_1/2 = -\mathcal{M}/2(\mathcal{M} + 1)$. This should be valid for systems having a very weakly bound state, where a new bound state just appears with the increasing \mathcal{M} . In Fig. 3(b) we also show the results estimated with Eq. (53) (blue dots) from the calculated bound-state energies for the systems having positive scattering lengths. They agree well with the results of accurate calculations even for rather tightly bound systems where the scattering length tends to be small, located at the middle parts between the jumps. For example, for $dd\mu$, Eq. (53) provides 2.9 m.a.u., which is about 60% of 5.1 m.a.u. from the accurate result.

The analysis can be repeated for all other regions of \mathcal{M} . Figure 4(a) shows the systems near H_2^+ . The jumps of 20 and 21 bound states occur at $\mathcal{M} = 1720$ – 1740 and 1900 – 1930 [see Fig. 4(b)], respectively. The locations of \mathcal{M} agree well with the values of 1730 and 1912 predicted by the BO approximation from Eqs. (51) and (52). Correspondingly, the scattering length jumps from $-\infty$ to ∞ around these values of \mathcal{M} and decreases monotonically during the range of \mathcal{M} having 20 bound states. The H_2^+ system is located at slightly larger side of \mathcal{M} from the center in the 20 bound-state region and the scattering length has a rather small negative value on the order of 10 m.a.u.

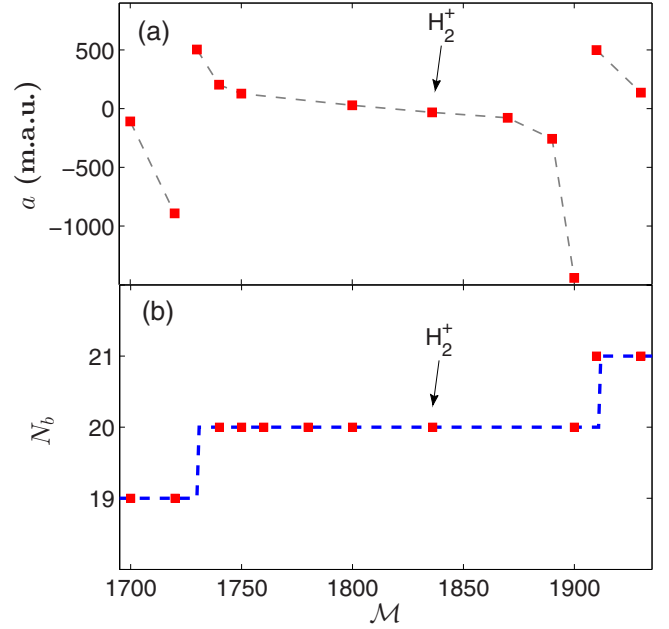


FIG. 4. (Color online) Same as Fig. 3 but for the systems with $1700 < \mathcal{M} \leq 2000$ including H_2^+ , which support 20 bound states below the dissociation threshold.

2. Odd permutation systems

The odd permutation symmetry states have attracted special interest in the theoretical studies of the symmetric Coulomb three-body systems. It has been known that the lowest BO potential for the odd states has a shallow minimum and there are two bound states in H_2^+ . The existence of the second bound state in H_2^+ was predicted in Ref. [59] and recently an accurate binding energy of $1.085\,045 \times 10^{-9}$ a.u. was obtained with a large size of the basis set [55]. This weakly bound state manifests itself as a huge scattering length of 715 m.a.u. (see Table III). It is of interest to study the mass ratio dependence of the scattering length and bound-state structures, in particular for the isotope systems of H_2^+ , D_2^+ , and T_2^+ . We are unaware of any data for those systems. Based on the analysis of the mass ratio dependence in the previous section, we expect that the scattering length and the number of bound states for D_2^+ and T_2^+ would be very different from those for H_2^+ . Figure 5 depicts the resulting $a(\mathcal{M})$ and $N_b(\mathcal{M})$ for several systems over the range of $0 < \mathcal{M} \leq 6000$ including D_2^+ and T_2^+ . It is shown that the scattering length jumps at $\mathcal{M} \sim 300$, 1700, and 4600, respectively. Correspondingly, $N_b(\mathcal{M})$ jumps around the same values of \mathcal{M} . We also plot the semiclassical approximation for N_b from Eqs. (51) and (52) with $\alpha = 0.1220$ for the odd BO potential. The semiclassical approximation underestimates the locations of the jumps by about $\sim 10\%$ in this region. The systems with $\mathcal{M} \lesssim 300$, such as H^- , Ps^- , $pp\mu$, $dd\mu$, and $tt\mu$, have no bound states. There are two bound states in H_2^+ and D_2^+ , but their scattering lengths are quite different. H_2^+ exists just above the second jump and has a large scattering length of 715 a.u. In contrast, D_2^+ is at slightly larger \mathcal{M} from the center of the second and the third jumps and thus it has a small negative scattering length of -45 a.u. Moving further in the larger \mathcal{M} side, T_2^+ is located in the middle part

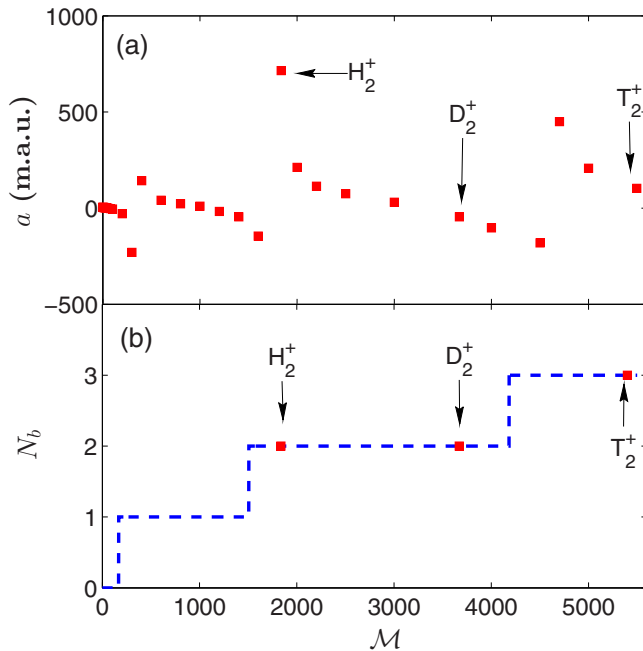


FIG. 5. (Color online) Same as Fig. 3 but for the systems with odd permutation symmetry in the range $0 < \mathcal{M} \leq 6000$.

between the third and fourth jumps, having three bound states. We carry out the bound-state calculations for D_2^+ and T_2^+ and obtain the binding energies of the highest bound states with respect to their dissociation thresholds: 1.4×10^{-6} and 4.6×10^{-8} a.u., respectively. Larger binding energies of D_2^+ and T_2^+ compared to that of H_2^+ can be understood by their smaller scattering lengths.

IV. CONCLUSION

Taking advantage of the HSE coordinate method, we have carried out calculations of ultralow-energy collisions for the symmetric Coulomb three-body systems with positive and negative unit charges with a mass ratio of constituting particles \mathcal{M} varying over several orders of magnitude. We have provided accurate results of the phase shifts as well as scattering lengths for prototypical systems of H^- , Ps^- , and H_2^+ and the scattering lengths for other exotic systems. Having the accurate calculations, we have investigated the scattering lengths systematically by changing \mathcal{M} nearly continuously. We have shown that the scattering length decreases monotonically from ∞ to $-\infty$ with increasing \mathcal{M} and jumps from $-\infty$ to ∞ at certain values of \mathcal{M} . This is closely related to the binding energy of the highest bound state of the system through Levinson's theorem. We also analyzed the mass ratio dependence of the scattering length a and the number N_b of bound states using a semiclassical approximation based on the BO picture. The jumps in the phase shifts as well as the number of bound states can be accurately estimated. We predicted the existence of the three bound states for odd permutation symmetry in T_2^+ and evaluated its bound-state energy accurately. Though the present calculations are focused on Coulomb three-body systems, this accurate and versatile procedure can be extended to various systems, which is very important in ultracold physics.

ACKNOWLEDGMENTS

This work was supported in part by JSPS KAKENHI Grants No. 26400415 and No. 10500598. Y.Z. thanks the JSPS for funding this research project. O.I.T. acknowledges support from the Russian Foundation for Basic Research (Grant No. 14-02-92110) and the Ministry of Education and Science of Russia (State Assignment No. 3.679.2014/K).

- [1] C. Schwartz, *Phys. Rev.* **124**, 1468 (1961).
- [2] J. Z. Tang, S. Watanabe, and M. Matsuzawa, *Phys. Rev. A* **46**, 2437 (1992).
- [3] T. Morishita, K.-i. Hino, S. Watanabe, and M. Matsuzawa, *Phys. Rev. A* **53**, 2345 (1996).
- [4] D. Kato and S. Watanabe, *Phys. Rev. A* **56**, 3687 (1997).
- [5] A. Igarashi and C. D. Lin, *Phys. Rev. Lett.* **83**, 4041 (1999).
- [6] H. Miyagi, T. Morishita, and S. Watanabe, *Phys. Rev. A* **85**, 022708 (2012).
- [7] S. J. Ward, J. W. Humberstonz, and M. R. C. McDowell, *J. Phys. B* **20**, 127 (1987).
- [8] C.-Y. Hu and A. A. Kvitsinsky, *Phys. Rev. A* **50**, 1924 (1994).
- [9] A. Igarashi, S. Nakazaki, and A. Ohsaki, *Phys. Rev. A* **61**, 032710 (2000).
- [10] A. Basu and A. S. Ghosh, *Phys. Rev. A* **72**, 062507 (2005).
- [11] O. I. Tolstikhin and C. Namba, *Phys. Rev. A* **60**, 5111 (1999), and references therein.
- [12] A. Dupays, *Phys. Rev. Lett.* **93**, 043401 (2004).
- [13] B. D. Esry and H. R. Sadeghpour, *Phys. Rev. A* **67**, 012704 (2003).
- [14] A. Martin, J.-M. Richard, and T. T. Wu, *Phys. Rev. A* **46**, 3697 (1992).
- [15] A. W. King, P. E. Herlihy, and H. Cox, *J. Chem. Phys.* **141**, 044120 (2014).
- [16] Z. Chen and C. D. Lin, *Phys. Rev. A* **42**, 18 (1990).
- [17] O. I. Tolstikhin, I. Y. Tolstikhina, and C. Namba, *Phys. Rev. A* **60**, 4673 (1999).
- [18] O. I. Tolstikhin, S. Watanabe, and M. Matsuzawa, *Phys. Rev. Lett.* **74**, 3573 (1995).
- [19] O. I. Tolstikhin and M. Matsuzawa, *Phys. Rev. A* **63**, 062705 (2001).
- [20] A. Schramm, J. M. Weber, J. Kreil, D. Klar, M. W. Ruf, and H. Hotop, *Phys. Rev. Lett.* **81**, 778 (1998).
- [21] T. Kraemer, M. Mark, P. Waldburger, J. G. Danzl, C. Chin, B. Engeser, A. D. Lange, K. Pilch, A. Jaakkola, H. C. Nägerl, and R. Grimm, *Nature (London)* **440**, 315 (2006).
- [22] M. Kurokawa, M. Kitajima, K. Toyoshima, T. Kishino, T. Odagiri, H. Kato, M. Hoshino, H. Tanaka, and K. Ito, *Phys. Rev. A* **84**, 062717 (2011).
- [23] H. Metcalf and P. van der Straten, *Phys. Rep.* **244**, 203 (1994).
- [24] S. Willitsch, M. T. Bell, A. D. Gingell, S. R. Procter, and T. P. Softley, *Phys. Rev. Lett.* **100**, 043203 (2008).
- [25] K. Tórkési, B. Juhász, and J. Burgdörfer, *J. Phys. B* **38**, S401 (2005).

- [26] C. I. Blaga, F. Catoire, P. Colosimo, G. G. Paulus, H. G. Muller, P. Agostini, and L. F. DiMauro, *Nat. Phys.* **5**, 335 (2009).
- [27] W. Quan, Z. Lin, M. Wu, H. Kang, H. Liu, X. Liu, J. Chen, J. Liu, X. T. He, S. G. Chen, H. Xiong, L. Guo, H. Xu, Y. Fu, Y. Cheng, and Z. Z. Xu, *Phys. Rev. Lett.* **103**, 093001 (2009).
- [28] Y. Zhou and C. Lin, *J. Phys. B* **27**, 5065 (1994).
- [29] A. Igarashi, I. Shimamura, and N. Toshima, *Phys. Rev. A* **58**, 1166 (1998).
- [30] B. Esry, H. Sadeghpour, E. Wells, and I. Ben-Itzhak, *J. Phys. B* **33**, 5329 (2000).
- [31] P. S. Krstić, J. H. Macek, S. Y. Ovchinnikov, and D. R. Schultz, *Phys. Rev. A* **70**, 042711 (2004).
- [32] E. Fermi, *Nuovo Cimento* **11**, 157 (1934).
- [33] C. H. Greene, A. S. Dickinson, and H. R. Sadeghpour, *Phys. Rev. Lett.* **85**, 2458 (2000).
- [34] E. Cornell and C. Wieman, *Rev. Mod. Phys.* **74**, 875 (2002).
- [35] V. Efimov, *Sov. J. Nucl. Phys.* **12**, 589 (1971).
- [36] S. Watanabe and H. Komine, *At. Collision Res. Jpn.: Prog. Rep.* **15**, 60 (1989).
- [37] O. I. Tolstikhin and H. Nakamura, *J. Chem. Phys.* **108**, 8899 (1998).
- [38] J. Macek, *J. Phys. B* **1**, 831 (1968).
- [39] C. D. Lin, *Phys. Rep.* **257**, 1 (1995).
- [40] O. I. Tolstikhin, S. Watanabe, and M. Matsuzawa, *J. Phys. B* **29**, L389 (1996).
- [41] K. Baluja, P. Burke, and L. Morgan, *Comput. Phys. Commun.* **27**, 299 (1982).
- [42] J. Wang, J. P. D’Incao, and C. H. Greene, *Phys. Rev. A* **84**, 052721 (2011).
- [43] H. Suno and B. D. Esry, *Phys. Rev. A* **89**, 052701 (2014).
- [44] M. Gailitis, *J. Phys. B* **9**, 843 (1976).
- [45] C. Noble and R. Nesbet, *Comput. Phys. Commun.* **33**, 399 (1984).
- [46] B. L. Christensen-Dalsgaard, *Phys. Rev. A* **29**, 2242 (1984).
- [47] I. Shimamura, *J. Phys. Soc. Jpn.* **30**, 1702 (1971).
- [48] A. K. Bhatia and A. Temkin, *Phys. Rev. A* **64**, 032709 (2001).
- [49] O. I. Tolstikhin, V. N. Ostrovsky, and H. Nakamura, *Phys. Rev. Lett.* **79**, 2026 (1997).
- [50] J. B. Delos, *Rev. Mod. Phys.* **53**, 287 (1981).
- [51] B. D. Esry and H. R. Sadeghpour, *Phys. Rev. A* **60**, 3604 (1999).
- [52] G. Hunter and M. Kuriyan, *Proc. R. Soc. London Ser. A* **353**, 575 (1977).
- [53] T. F. O’Malley, L. Rosenberg, and L. Spruch, *Phys. Rev.* **125**, 1300 (1962).
- [54] E. Bodo, P. Zhang, and A. Dalgarno, *New J. Phys.* **10**, 033024 (2008).
- [55] J. Carbonell, R. Lazauskas, D. Delande, L. Hilico, and S. Kilic, *Europhys. Lett.* **64**, 316 (2003).
- [56] N. Levinson, K. Dan, *Vidensk. Selsk. Mat. Fys. Medd.* **25**, 9 (1949).
- [57] R. Newton, *Scattering Theory of Waves and Particles* (Springer, New York, 1982).
- [58] L. D. Landau and E. M. Lifshitz, *Quantum Mechanics (Nonrelativistic Theory)* (Pergamon, Oxford, 1977).
- [59] J. Peek, *J. Chem. Phys.* **50**, 4595 (1969).